Genes & Diseases (2023) 10, 2195–2198

Available online at www.sciencedirect.com

ScienceDirect

journal homepage: www.keaipublishing.com/en/journals/genes-diseases

RAPID COMMUNICATION

Targeting hypoxia-induced CBS expression inhibits breast cancer stem cells through the induction of ferroptosis

Triple-negative breast cancer (TNBC) has a poor prognosis because of its aggressive characteristics and lack of targeted therapies.[1] Recently, it has been reported that TNBC is sensitive to ferroptosis, an iron-dependent type of programmed cell death, making it a potential target for the treatment of TNBC.[2] Breast cancer stem cells (BCSCs), a small population of cancer cells that possess the infinite proliferative potential and tumor-initiating properties, play important roles in drug resistance.[3] The responses of BCSCs to ferroptosis-inducing agents are controversial and remain elusive.

Intratumoral hypoxia (lack of oxygen) is a common feature of breast cancer and promotes BCSC maintenance and specification via multiple pathways dependent on hypoxia-inducible factors (HIFs), which are the master regulators of O_2 homeostasis.[4] We first investigated the effect of hypoxia on ferroptosis by treating TNBC cell lines MDA-MB-231, SUM159, and Hs578T with cystine transporter xCT inhibitor erastin (Era) or sulfasalazine (SSA) under 20% or 1% of oxygen concentration for 48 h. Both agents reduced cell viability by >50% through ferroptosis in all three TNBC cell lines under 20% of oxygen but failed to induce ferroptosis under 1% of oxygen (Fig. 1A; Fig. S1A, B). Erastin treatment increased lipid peroxidation, a hallmark of ferroptosis,[5] under 20% but not 1% of oxygen (Fig. 1A). Knockdown of HIF-1α, but not HIF-2α, re-sensitized TNBC cell lines to xCT inhibitor-induced ferroptosis, and erastin-induced lipid peroxidation (Fig. 1B; Fig. S1C), under 1% of oxygen, indicating that hypoxia mediates ferroptosis resistance in a HIF-1-dependent manner in TNBC.

We found that xCT inhibitors decreased cystine uptake at similar levels under 20% or 1% of oxygen (Fig. S2A). However, the xCT inhibitor-mediated decrease of intracellular glutathione levels was largely blocked under 1% of oxygen (Fig. S2B). Thus, we hypothesized that TNBC cells may employ cystathionine, which is combined from homocysteine and serine catalyzed by the enzyme CBS (cystathionine beta-synthase) (Fig. 1C), as an alternative cysteine source for the synthesis of glutathione to protect against ferroptosis under hypoxic condition when cystine uptake is blocked. We found that hypoxic exposure induced CBS mRNA and protein levels in TNBC cell lines, which was abrogated by HIF-1α knockdown (Fig. 1D, E; Fig. S3A) or HIF-1 inhibitor digoxin (Fig. S3B). Daily treatment with 2 mg/kg digoxin decreased CBS mRNA expression in a xenograft mouse model implanted with MDA-MB-231 cells, and in a genetically engineered autochthonous MMTV-PyMT breast cancer mouse model (Fig. 1F). Gene expression analysis from 1097 human breast cancer specimens in The Cancer Genome Atlas (TCGA) database revealed a significant correlation ($r = 0.34$, $P < 0.0001$) of CBS mRNA levels with a HIF-metagene signature (Fig. 1G; Fig. S3C) and significantly higher CBS expression in the basal-like subtype of breast cancers (Fig. S3C, D). All these data indicate that CBS expression is regulated by HIF-1.

We performed ChIP (chromatin immunoprecipitation)-qPCR assay and confirmed that HIF-1α and HIF-1β directly bind to a site located in the 5′-flanking region of *CBS* gene (Fig. 1H; Fig. S3E). We also generated a reporter plasmid by inserting a 55-bp oligonucleotide spanning the HIF-1 binding site into the pGL2-promoter reporter plasmid and performed a luciferase reporter assay to confirm this binding site is a functional hypoxia response element (HRE) (Fig. 1I; Fig. S3F). These data indicate that hypoxia induces HIF-1-dependent transactivation of *CBS*.

To investigate the role of CBS in hypoxia-mediated ferroptosis resistance, we generated CBS knockdown subclones in TNBC cells (Fig. S4A) and found that CBS knockdown re-sensitized TNBC cells for erastin- or sulfasalazine-decreased glutathione levels under 1% O_2, which

Peer review under responsibility of Chongqing Medical University.

https://doi.org/10.1016/j.gendis.2023.02.034

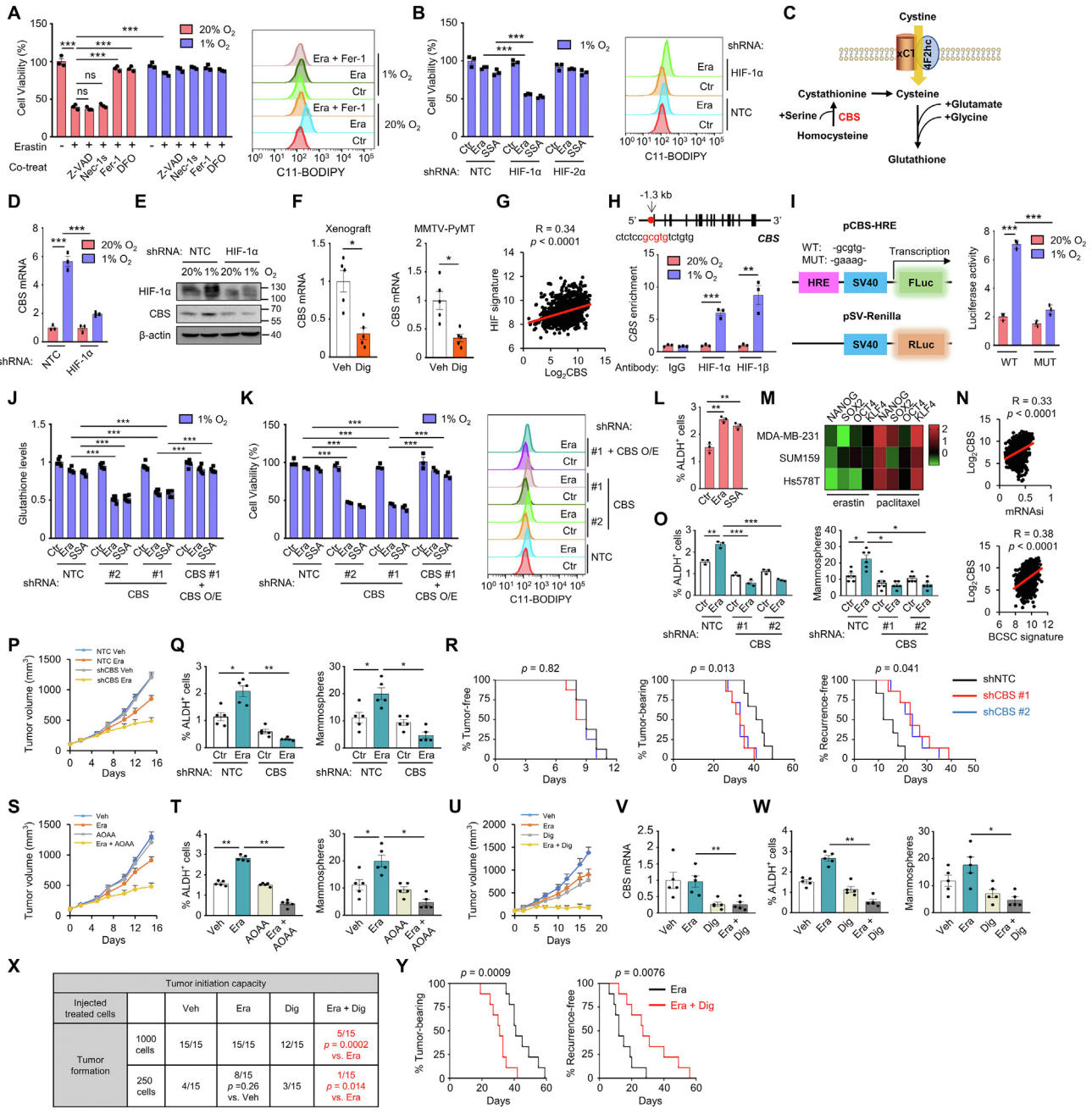

Figure 1 Targeting hypoxia-induced CBS expression inhibits breast cancer stem cells through the induction of ferroptosis. **(A, B)** MDA-MB-231 cells (A) or knockdown subclones (B) were treated as indicated under 20% or 1% O_2 for 48 h. MTT assays were performed to measure cell viability (left) and C11-BODIPY staining was performed followed by flow cytometry to measure lipid peroxidation (right). **(C)** A scheme of intracellular cysteine sources. **(D, E)** MDA-MB-231 subclones were exposed to 20% or 1% O_2 for 24 h, and RT-qPCR (D) and immunoblot (E) assays were performed. **(F)** Xenograft mice were implanted with MDA-MB-231 cells (left), or MMTV-PyMT transgenic mice (right) were treated with vehicle (Veh) or digoxin (Dig, 2 mg/kg daily for 15 days), and tumors were harvested on day 15 for RT-qPCR. **(G)** CBS mRNA levels in each of 1097 human primary breast cancers from the TCGA database were compared with the HIF signature using Pearson's correlation test. **(H)** MDA-MB-231 cells were exposed to 20% or 1% O_2 for 16 h, and ChIP was performed followed by qPCR with primers flanking the candidate HIF binding site in the *CBS* gene. **(I)** MDA-MB-231 cells were co-transfected with pCBS-HRE (WT or MUT), which contains a 55-bp candidate HRE upstream of an SV40 promoter and firefly luciferase coding sequences, and pSV-Renilla, a control plasmid containing Renilla luciferase coding sequences downstream of the SV40 promoter. At 24 h post-transfection, cells were exposed to 20% or 1% O_2 for 24 h, and Firefly:Renilla ratio was determined. **(J, K)** MDA-MB-231 subclones were treated with erastin (Era) or sulfasalazine (SSA) under 1% O_2 for 48 h and intracellular glutathione levels (J), cell viability (K, left), and lipid peroxidation (K, right) were measured. **(L)** MDA-MB-231 cells were treated with Era or SSA for 72 h and the percentage of $ALDH^+$ cells was determined. **(M)** TNBC cells were treated with vehicle, erastin, or paclitaxel for 72 h qPCR assays were performed, $\log_2$ (fold change) of erastin or paclitaxel treated *vs.* vehicle was calculated, and a heatmap was

was rescued by overexpression of short hairpin RNA (shRNA)-resistant CBS vector (Fig. 1J; Fig. S4A, B), indicating an important role of CBS in the maintenance of intracellular glutathione levels when cystine uptake is inhibited. CBS knockdown also increased erastin-induced lipid peroxidation and re-sensitized TNBC cells to xCT inhibitor-mediated cell death under 1% O_2, both of which were rescued by shRNA-resistant CBS vector overexpression (Fig. 1K; Fig. S4A, C). These data demonstrate the critical role of CBS in ferroptosis resistance under hypoxic condition.

Next, we investigated the biological consequence of CBS-mediated ferroptosis resistance in breast cancer therapeutics. BCSCs are resistant to drug treatment and are majorly located in hypoxic niches. Erastin or sulfasalazine treatment increased the percentage of $ALDH^+$ cell population that have BCSC characteristics (Fig. 1L; Fig. S5A, B). Unlike the chemotherapeutic agent paclitaxel, which induces BCSC enrichment through active induction of pluripotency factor expression, erastin treatment failed to increase the expression of pluripotency factors (Fig. 1M), which are required for active conversion of non-BCSCs to BCSCs, suggesting that BCSC resistance to erastin-mediated ferroptosis is the major cause of erastin-induced BCSC enrichment. Thus, we hypothesized that CBS contributes to ferroptosis resistance in BCSCs.

CBS expression was dramatically increased in the BCSC-enriched $ALDH^+$ population (Fig. S5C) and nonadherent mammospheres (Fig. S5D). CBS mRNA level in primary breast cancer patients from the TCGA database was correlated with breast cancer stemness, as measured by an mRNA expression-based stemness index (mRNAsi) generated through machine learning, and by the expression of a 20-gene BCSC signature (Fig. 1N), suggesting a correlation between CBS expression and the BCSC phenotype. CBS knockdown completely abolished erastin-mediated increases in the percentage of $ALDH^+$ cells and the number of mammosphere-forming cells (Fig. 1O; Fig. S5E, F), indicating that CBS knockdown sensitizes BCSCs to erastin-mediated ferroptosis.

To investigate the role of CBS in the regulation of ferroptosis resistance in BCSCs *in vivo*, we implanted MDA-MB-231 NTC (nontargeting control) or CBS-knockdown subclone cells in severe combined immunodeficiency (SCID) mice. CBS knockdown did not affect tumor growth rate but sensitized tumors to erastin treatment (Fig. 1P). Erastin treatment increased the percentage of $ALDH^+$ cells and the number of mammosphere-forming cells, which were completely abolished by CBS knockdown (Fig. 1Q; Fig. S6A).

To determine the effects of CBS on BCSC population after erastin treatment *in vivo*, we injected MDA-MB-231 NTC or CBS-knockdown subclone cells and performed tumor eradication assay by treating the mice with 20 mg/kg erastin every day, terminated erastin treatment when tumors were no longer palpable and monitored tumor recurrence. CBS knockdown did not alter the time to tumor formation but decreased the time to tumor eradication. Most importantly, CBS knockdown markedly prolonged the time to tumor recurrence after erastin treatment was terminated (Fig. 1R), indicating a decreased BCSC population in CBS-knockdown subclones compared with NTC after erastin treatment *in vivo*.

We next investigated whether pharmacological inhibition of CBS reverses ferroptosis resistance in BCSCs. Co-administration of CBS inhibitor AOAA (aminooxyacetic acid) with erastin reversed hypoxia-induced ferroptosis resistance (Fig. S7A) and increased lipid peroxidation under 1% O_2 (Fig. S7B) *in vitro*. In xenograft mice with MDA-MB-231, co-administration of AOAA increased the inhibitory effect of erastin on tumor growth (Fig. 1S), and completely abolished erastin-induced increase of the percentage of $ALDH^+$ cells and mammosphere-forming cells (Fig. 1T; Fig. S8A). These data demonstrate that genetic or pharmacological inhibition of CBS decreases ferroptosis resistance in BCSCs *in vivo*.

To explore the translational implications of our findings, we investigated whether the HIF-1 inhibitor digoxin, which is under clinical trials for the treatment of breast cancer, targets BCSCs through CBS inhibition *in vivo*. Co-administration of digoxin with erastin markedly inhibited tumor growth (Fig. 1U), decreased CBS mRNA levels (Fig. 1V), and completely abolished erastin-induced increase of the percentage of $ALDH^+$ cells and the number of mammosphere-forming cells (Fig. 1W; Fig. S9A), demonstrating that

plotted. **(N)** Pearson's test was used to analyze the correlation of CBS mRNA expression with mRNAsi (top) and BCSC signature (bottom) in human primary breast cancers from the TCGA database. **(O)** MDA-MB-231 subclone cells were treated with Era for 72 h and the percentage of $ALDH^+$ cells (left) and the number of mammospheres per 1000 cells seeded (right) were determined. **(P, Q)** SCID mice were injected with 2×10^6 MDA-MB-231 NTC or CBS-knockdown subclone cells and treated with saline or 20 mg/kg Era daily for 15 days. Tumor volumes were measured every 2–3 days (P). Tumor samples were harvested on day 15 for ALDH and mammosphere assays (Q). **(R)** 2×10^6 MDA-MB-231 NTC or CBS-knockdown subclone cells were implanted into SCID mice. When tumors became palpable, mice were treated with 20 mg/kg Era daily until tumors were no longer palpable. Kaplan–Meier survival curves of tumor-free (left), tumor-bearing (center), and recurrence-free (right) were plotted. **(S, T)** SCID mice were injected with 2×10^6 MDA-MB-231 cells and treated with saline, Era (20 mg/kg daily), AOAA (10 mg/kg daily), or Era plus AOAA, for 15 days. Tumor volumes were measured every 2–3 days (S). Tumor samples were harvested on day 15 for ALDH and mammosphere assays (T). **(U–W)** SCID mice were injected with 2×10^6 MDA-MB-231 cells and treated with saline, Era (20 mg/kg daily), Dig (2 mg/kg daily), or Era plus Dig, for 15 days. Tumor volumes were measured every 2–3 days (U). Tumor samples were harvested on day 15 for qPCR (V), ALDH (W, left), and mammosphere (W, right) assays. **(X)** MDA-MB-231 cells were pre-treated with Veh, Era, Dig, or Era plus Dig for 48 h and live cells were counted and implanted into SCID mice (1,000 or 250 live cells each). The number of mice that developed a tumor after 10 weeks is shown, and Fisher exact test was performed to determine statistical significance. **(Y)** MDA-MB-231 cells were implanted into SCID mice (2×10^6 per mouse). When tumors became palpable, mice were treated with 20 mg/kg Era, or 20 mg/kg Era plus 2 mg/kg Dig daily until tumors were no longer palpable. Kaplan–Meier survival curves of tumor-bearing (left) and recurrence-free (right) were plotted and *P* values of log-rank tests are shown. $^*P < 0.05$, $^{**}P < 0.01$, $^{***}P < 0.001$.

pharmacological inhibition of HIF-1 induces ferroptosis not only in bulk cells but also in BCSCs.

To examine the role of HIF-1 inhibitor in the induction of ferroptosis specifically in BCSCs, we performed *in vivo* tumorigenicity assay to measure the number of BCSCs after treatment. We treated MDA-MB-231 cells with erastin, alone or in combination with digoxin, counted the number of live cells, and injected 1,000 or 250 live cells into SCID mice so that BCSCs were limiting for tumor formation. We found that co-administration of digoxin completely abolished (or even further decreased) erastin-induced BCSC enrichment (Fig. 1X). We also examined the effect of HIF-1 inhibitor on BCSCs *in vivo* through tumor eradication assay, and found that co-treatment with digoxin made tumors more sensitive to erastin treatment, as measured by the decreased time to tumor eradication, and markedly inhibited tumor relapse, as measured by the increased time to tumor recurrence (Fig. 1Y). These data demonstrate that pharmacological inhibition of HIF-1, which decreases CBS expression, sensitizes BCSCs to ferroptosis and inhibits the BCSC population.

In summary, we demonstrate that TNBC cells develop ferroptosis resistance through HIF-1-induced CBS up-regulation, which provides an alternative cysteine source for the synthesis of glutathione and protects cells against ferroptosis induced by cystine uptake inhibition. CBS is overexpressed in BCSCs and mediates the resistance of BCSCs to ferroptosis. A caveat of this study is that we did not provide direct evidence of ferroptosis in BCSCs *in vivo* because of the technical difficulty, considering the small percentage of BCSCs in the bulk tumor. This study provides compelling evidence that targeting the HIF-1-CBS pathway in combination with ferroptosis-inducing agents may effectively inhibit BCSCs and thereby improve clinical outcomes for TNBC patients.

Author contributions

G.W., J.L., J.L., R.S., C.Z., and H.L. designed the research study. G.W., J.L., J.L., G.J., H.X., and Z.Z. performed experiments and acquired data. G.J., H.X., and C.Z. performed database analyses. G.W., J.L., and H.X. performed statistical analyses. G.W., J.L., J.L., G.J., Z.Y., R.S., C.Z., and H.L. analyzed the data and wrote the manuscript. C.Z. and H.L. supervised the study. All authors reviewed and commented on the manuscript.

Conflict of interests

The authors declare no competing interests.

Funding

This work was supported by the Natural Science Foundation of Shandong Province, China (No. ZR2021YQ50, Excellent Young Scholars Program), National Natural Science Foundation of China (No. 82003227), China Postdoctoral Science Foundation (No. 2019M663516 and 2021T140487), Post-Doctor Research Project, Sichuan University, China (No. 2020SCU12021), Post-Doctor Research Project, West China Hospital, Sichuan University, China (No. 2018HXBH067), and Sichuan Provincial Research Foundation for Basic Research (China) (No. 2020YFS0272). H.L. is the Taishan Scholar Young Talent Professor of Shandong Province, China, and the Cheeloo Young Talent Professor at Shandong University.

Appendix A. Supplementary data

Supplementary data to this article can be found online at https://doi.org/10.1016/j.gendis.2023.02.034.

References

1. Foulkes WD, Smith IE, Reis-Filho JS. Triple-negative breast cancer. *N Engl J Med*. 2010;363(20):1938—1948.
2. Doll S, Proneth B, Tyurina YY, et al. ACSL4 dictates ferroptosis sensitivity by shaping cellular lipid composition. *Nat Chem Biol*. 2017;13(1):91—98.
3. Zheng Q, Zhang M, Zhou F, et al. The breast cancer stem cells traits and drug resistance. *Front Pharmacol*. 2020;11:599965.
4. Semenza GL. The hypoxic tumor microenvironment: a driving force for breast cancer progression. *Biochim Biophys Acta*. 2016;1863(3):382—391.
5. Dixon SJ, Stockwell BR. The hallmarks of ferroptosis. *Annu Rev Cancer Biol*. 2019;3:35—54.

Guangyao Wei [a,b,1], Jia Liu [a,b,1], Jie Lan [c,1], Guangyu Ji [a,b], Huize Xia [a,b], Zhiqun Zhao [a,b], Zhaoxue Yu [d], Rong Sun [a], Chuanzhao Zhang [e,**], Haiquan Lu [a,b,d,f,*]

[a] *The Second Hospital and Advanced Medical Research Institute, Cheeloo College of Medicine, Shandong University, Jinan, Shandong 250012, China*
[b] *Key Laboratory for Experimental Teratology of the Ministry of Education, Cheeloo College of Medicine, Shandong University, Jinan, Shandong 250012, China*
[c] *Department of Radiation Oncology, Cancer Center and State Key Laboratory of Biotherapy, West China Hospital, Sichuan University, Chengdu, Sichuan 610041, China*
[d] *Shandong Zhongke Institute for Regenerative Medicine, Jinan, Shandong 250012, China*
[e] *Department of General Surgery, Guangdong Provincial People's Hospital, Guangdong Academy of Medical Sciences, Guangzhou, Guangdong 510080, China*
[f] *Center for Reproductive Medicine, Cheeloo College of Medicine, Shandong University, Jinan, Shandong 250012, China*

*Corresponding author. Room 211, Building 10, No.17922 Jingshi Road, Jinan, Shandong 250012, China.

**Corresponding author. No. 106 Zhongshan 2nd Road, Guangzhou, Guangdong 510080, China.
E-mail addresses: zhangchuanzhao@gdph.org.cn (C. Zhang), lvhaiquan@sdu.edu.cn (H. Lu)

18 July 2022
Available online 28 March 2023

[1] These authors contributed equally to this work.